Improving Energy-Efficiency of HFC Networks with a Master-Slave Linecard Configuration

Yabo Yuan[1], Ping Lu[1], Joel J. P. C. Rodrigues[2], Zuqing Zhu[1,†]

[1]School of Information Science and Technology, University of Science and Technology of China, Hefei, China
[2]Department of Informatics, University of Beira Interior, Portugal
[†]Email: {zqzhu}@ieee.org

Abstract—We develop a novel traffic scheduling algorithm based on a master-slave linecard (LC) configuration to improve the energy-efficiency of hybrid fiber-coaxial (HFC) networks. The algorithm forwards packets to the master or slave LC adaptively according to the traffic load, and toggles the LCs between working and sleeping modes for energy-saving. To optimize the algorithm's key parameters, we model the system using a two-dimensional Markov process and derive the analytical expressions of several performance metrics, including average packet delay, LC switching frequency, and energy efficiency improvement. We then verify the theoretical analysis with numerical simulations using the Monte Carlo method. Both the theoretical and simulation results indicate that the proposed algorithm can achieve significant energy efficiency improvement, while keeping the average packet delay and LC switching frequency low.

Index Terms—Hybrid fiber-coaxial (HFC) networks, Energy-efficient scheduling, Master-slave linecard configuration, Energy-delay tradeoff

I. INTRODUCTION

Nowadays, the increasing speed of equipment installations makes the Internet's energy consumption a global concern. A recent study on network energy consumption growth indicated that access networks were among top carbon emission contributors in the Internet [1]. Moreover, this situation will not change in the short-to-middle-term future, as the service providers are investing heavily in broadband access networks to facilitate sufficient bandwidth for new network applications, such as video-on-demand, tele-conferencing, video gaming and etc. To this end, many energy-saving techniques have been proposed for various types of access networks, including mobile access networks [2], passive optical networks (PON) [3], hybrid wireless-optical broadband access networks (WOBAN) [4], digital subscriber line (DSL) networks [5], and hybrid fiber-coaxial (HFC) networks [6, 7]. HFC networks provide Internet data services over the existing cable television (TV) systems, which have an hybrid infrastructure that combines optical fibers and coaxial cables and deliver digitally modulated signals through RF TV channels. Since this type of access networks have the second biggest user population globally among all wired ones [8], it is worth developing energy-saving techniques to reduce both the operational expenditure (OPEX) and the environmental impacts.

As the industry standard for developing HFC equipments, Data over Cable Service Interface Specifications (DOCSIS) [9] define two primary types of HFC network equipments,

i.e., the cable modem terminal system (CMTS) located at an operator's headend, and the cable modems (CMs) at customer premises. Recently, DOCSIS 3.0 [10] has been released. It includes channel-bonding as a major technology improvement, which can provide cable operators a remarkable opportunity to outpace competitors such as fiber-to-the-home (FTTH) providers. Specifically, DOCSIS 3.0 allows a CM to groom multiple RF channels from the CMTS as a virtual broadband channel for data transmission at 100 Mb/s or more. Even though it can boost up customers' access data-rates effectively, channel bonding also causes significant power consumption increase in HFC networks. For instance, a CMTS linecard (LC) has to be designed with an increased number of ports, which makes it more power-hungry.

Previously, we have reported several energy-saving algorithms for the HFC networks based on DOCSIS 3.0 [6, 7]. In [6], we considered the operations of a CMTS and CMs jointly and proposed an approach for cooperative energy-saving. In [7], we studied traffic scheduling in channel-bonding CMs, and formulated an analytical model to investigate the energy-delay tradeoff. From the perspective of a CMTS chassis, multiple versions of LCs can co-exist. Although equipping the most advanced version of LCs in all slots of a CMTS chassis can boost its capacity to the highest, the capital expenditure (CAPEX) associated with the LC replacements and the OPEX caused by the energy bills can be prohibitively high. Recently, in [11], Parker *et al.* proposed a master-slave router configuration for energy-saving in optical networks. A CMTS chassis can also incorporate a similar configuration and toggles between a master and a slave LCs for energy-saving. However, to make the master-slave configuration work efficiently in a CMTS, we still need to develop a traffic scheduling algorithm that considers the characteristics of HFC networks and to investigate the tradeoffs between energy efficiency and other performance metrics, such as average packet delay and LC switching frequency.

In this paper, we develop a novel energy-efficient traffic scheduling algorithm based on the master-slave LC configuration in a CMTS. The algorithm forwards packets to the master or slave LC adaptively according to the traffic load, and toggles the LCs between working and sleeping modes for energy-saving. To understand the performance impacts of the algorithm's key parameters, we model the system using a two-dimensional Markov process and derive the analytical

expressions of a few performance metrics, including average packet delay, LC switching frequency, and energy efficiency improvement. The theoretical analysis is then verified by numerical simulations using the Monte Carlo method. We also investigate the tradeoffs between the performance metrics to further optimize the algorithm.

The rest of the paper is organized as follows. Section II explains the system model and illustrates the operation principle of the proposed algorithm. In Section III, we show the theoretical analysis. The performance evaluations are described in Section IV. Finally, Section V summarizes the paper.

II. SYSTEM MODEL

Fig.1 shows the system model of the master-slave configuration of two LCs in a CMTS chassis. Notice that a CMTS chassis usually accommodates more than two LCs and the rest of the LCs can operate independently from these two. In the context of this work, we assume that the upstream (US) capacities (*i.e.*, the traffic capacity from CMs to a CMTS LC) of the master and slave LCs are identical, but the master LC's downstream (DS) capacity (*i.e.*, the traffic capacity from a LC to CMs) is larger than that of the slave one. This assumption is valid since the traffic of HFC networks is asymmetric [12] and the DS provision speed of a CM is normally larger. Hence, we can trigger LC switching based on DS traffic only.

We assume that DS packets arrive at the CMTS following the Poisson process with a rate λ. The packets are then buffered in a finite queue q. We denote the length of the queue as N, in terms of number of packets. The number of pending packets in the queue is defined as $L(t)$ for a time instant t. We assume the service time per packet on the two LCs follows the exponential distribution, where the mean values are denoted as $1/\mu_m$ and $1/\mu_s$ ($\mu_m > \mu_s$), for the master and slave LCs, respectively. The energy-efficient scheduling algorithm determines the operation modes of the LCs based on $L(t)$, and forwards packets to a proper LC. In a practical CMTS system, traffic switching between two LCs can be realized with the high-availability feature [13]. The scheduling algorithm operates based on the definitions as follows.

Definition 1 (LC Operation Modes). We define two operation modes for a linecard: 1) Working, as it is turned on for transmitting data. The average power consumptions of the master and slave LCs in this mode are denoted as P_m and P_s ($P_m > P_s$), respectively. 2) Sleeping, as it is in the energy-saving mode with an average power consumption of P_0.

We assume that the power consumption P of a CMTS LC increases sub-linearly with its capacity μ [14],

$$P = \alpha \cdot \mu^{2/3} \qquad (1)$$

where α is a constant coefficient, and μ is the LC's capacity. Then, we get $P_m = \alpha(\mu_m)^{2/3}$ and $P_s = \alpha(\mu_s)^{2/3}$.

Definition 2 (Traffic Queue Sampling Period). The scheduling algorithm samples the traffic queue q with a random period T_s that follows an exponential distribution. The average value of T_s is denoted as S.
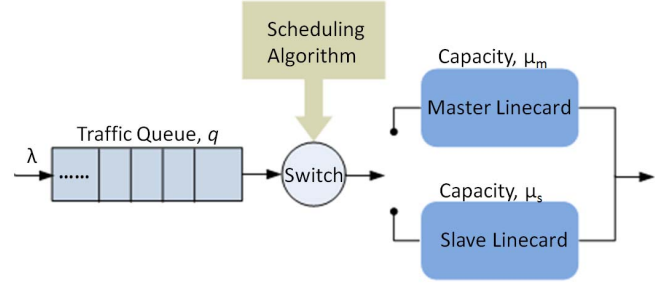

Fig. 1. System model for master-slave linecard configuration.

Definition 3 (Linecard Switching Threshold). When a sampling period expires, the scheduling algorithm examines the length of the queue, $L(t)$. When $L(t) > \mu_s + \varepsilon$, the master LC will be put into the working mode; otherwise, when $L(t) \leq \mu_s - \varepsilon$, the algorithm will toggle traffic transmission to the slave LC. Here, ε is a parameter that we use to optimize the algorithm for avoiding excessive LC switchings. To maximize energy-saving, we also assume that when the master LC becomes idle during the working mode ($L(t) = 0$), it notices the scheduler to invoke a LC switching.

Algorithm 1 illustrates the details of the proposed scheduling algorithm. We assume that the switching transition is negligible since it is usually much smaller than S in a practical CMTS system.

Algorithm 1 Energy-Efficient Scheduling for Master-Slave Configuration

---
1: **while** system is operational **do**
2:     measure $L(t)$;
3:     **if** $L(t) > \mu_s + \varepsilon$ **then**
4:       **if** slave LC is in working mode **then**
5:         invoke a LC switch: slave $\mapsto$ master;
6:         put slave LC into sleeping mode;
7:       **end if**
8:     **else if** $L(t) \leq \mu_s - \varepsilon$ **then**
9:       **if** master LC is in working mode **then**
10:        invoke a LC switch: master $\mapsto$ slave;
11:        put master LC into sleeping mode;
12:       **end if**
13:     **end if**
14:     determine the next queue sampling period T_s;
15:     $wait(T_s)$;
16: **end while**

III. THEORETICAL ANALYSIS

A. Infinitesimal Generator Matrix $\mathbb{Q}$

We model the system discussed above with a two-dimensional Markov process $\{(L(t), K(t)), t > 0\}$, where $L(t)$ is the pending packets in the queue, and $K(t)$ identifies the LCs' state, with $K(t) = 1$ and $K(t) = 2$ represent the state of {master←working, slave←sleeping}

and {master←sleeping, slave←working}, respectively. For the Markov process, we define the subset of the states that have a same $L(t)$ as a level, denoted as $\ell(L(t))$. Hence, the state space can be written as $\bigcup\limits_{i\in[0,N]} \ell(i)$, where

$$\ell(i) = \begin{cases} \{(0,2)\}, & i = 0 \\ \{(i,1),(i,2)\}, & i = 1,...,N \end{cases}$$

We define the traffic load as the ratio between λ and μ_m, i.e., $\rho = \lambda/\mu_m$. The infinitesimal generator matrix $\mathbb{Q}$ of the Markov process can be written as:

$$\mathbb{Q} = \begin{bmatrix} B_0 & C_0 & & & \\ A_1 & B_1 & C_1 & & \\ & \ddots & \ddots & \ddots & \\ & & A_{N-1} & B_{N-1} & C_{N-1} \\ & & & A_N & B_N \end{bmatrix} \quad (2)$$

where the sub-matrix A_i denotes the backward transition rates from level $\ell(i)$ to $\ell(i-1)$, sub-matrix B_i is for the local transition rates within level $\ell(i)$, and sub-matrix C_i is for the forward transition rates from level $\ell(i)$ to $\ell(i+1)$. These sub-matrices can be derived as follows with $\theta = 1/S$,

$$A_i = \begin{cases} \begin{bmatrix} \mu_m \\ \mu_s \end{bmatrix}, & i = 1 \\ \\ \begin{bmatrix} \mu_m & \\ & \mu_s \end{bmatrix}, & i \in (1, N] \end{cases} \quad (3)$$

$$B_i = \begin{cases} -\lambda, & i = 0 \\ \begin{bmatrix} -\lambda - \mu_m - \theta & \theta \\ & -\lambda - \mu_s \end{bmatrix}, & i \in (0, \mu_s - \varepsilon] \\ \begin{bmatrix} -\lambda - \mu_m & \\ & -\lambda - \mu_s \end{bmatrix}, & i \in (\mu_s - \varepsilon, \mu_s + \varepsilon] \\ \begin{bmatrix} -\lambda - \mu_m & \\ \theta & -\lambda - \mu_s - \theta \end{bmatrix}, & i \in (\mu_s + \varepsilon, N-1] \\ \begin{bmatrix} -\mu_m & \\ \theta & -\mu_s - \theta \end{bmatrix}, & i = N \end{cases} \quad (4)$$

$$C_i = \begin{cases} \begin{bmatrix} 0 & \lambda \end{bmatrix}, & i = 0 \\ \begin{bmatrix} \lambda & \\ & \lambda \end{bmatrix}, & i \in (0, N-1] \end{cases} \quad (5)$$

B. Matrix Geometric Solution

We define the steady probabilities of the Markov process as $\boldsymbol{\pi}$,

$$\boldsymbol{\pi} = (\pi_0, \boldsymbol{\pi_1}, \ldots, \boldsymbol{\pi_i}, \ldots, \boldsymbol{\pi_N}) \quad (6)$$

with $\boldsymbol{\pi_i}$ as the row-vector of the steady probabilities of level $\ell(i)$,

$$\boldsymbol{\pi_i} = \begin{cases} \pi_{0,2}, & i = 0 \\ \begin{bmatrix} \pi_{i,1} & \pi_{i,2} \end{bmatrix}, & i \in (0, N] \end{cases}$$

It is known that the Markov process can satisfy [15],

$$\boldsymbol{\pi}\mathbb{Q} = \mathbf{0} \quad (7)$$

and the row-vectors $\{\boldsymbol{\pi_i}\}$ should make sure that the summation of the steady probabilities equals 1,

$$\sum_{i=0}^{N} \boldsymbol{\pi_i}\mathbf{1} = 1 \quad (8)$$

where $\mathbf{1}$ is a column-vector of 1's. Then, by combining Eqns. (2-8), $\boldsymbol{\pi_i}$ can be analytically expressed with ρ, μ_m, μ_s, ε, and S.

C. Performance Metrics

In this Subsection, we provide the analytical expressions of several system performance metrics, including average packet delay, LC switching frequency, and energy efficiency improvement based on the above theoretical analysis.

1) Average Packet Delay: According to the Little's Law, the average packet delay can be obtained as

$$\overline{D} = \frac{\sum\limits_{i=1}^{N}\sum\limits_{k=1}^{2} i \cdot \pi_{i,k}}{\rho \cdot \mu_m(1 - \sum\limits_{k=1}^{2}\pi_{N,k})} \quad (9)$$

2) Linecard Switching Frequency: The LC switching frequency f can be derived as,

$$f = \frac{\sum\limits_{i=\lceil \mu_s+\varepsilon+1\rceil}^{N}\pi_{i,2} + \sum\limits_{i=1}^{\lfloor \mu_s-\varepsilon\rfloor}\pi_{i,1} + S \cdot \mu_m \cdot \pi_{1,1}}{S} \quad (10)$$

3) Energy Efficiency Improvement: The energy-efficient improvement η, can be calculated as,

$$\begin{aligned} \eta &= 1 - \frac{P_{energy-saving}}{P_{normal}} \\ &= 1 - \frac{P_m \sum\limits_{i=1}^{N}\pi_{i,1} + P_s \sum\limits_{i=0}^{N}\pi_{i,2} + P_0}{P_m} \end{aligned} \quad (11)$$

TABLE I
SIMULATION PARAMETERS

N, System queue length	10000 packets
μ_m, Master LC's service rate per time unit	100 packets
μ_s, Slave LC's service rate per time unit	1 - 100 packets
P_m, Master LC's average power in working mode	1 power-unit
P_0, A LC's power in sleeping mode	0 power-unit
ρ, Traffic load	0 - 1

IV. PERFORMANCE EVALUATIONS AND ALGORITHM OPTIMIZATIONS

We perform Monte Carlo simulations with 1000 time instants to verify the theoretical analysis discussed above and to evaluate the impacts of the algorithm's parameters, including the capacity ratio between the master and slave LCs $\gamma = \mu_s/\mu_m$, the average traffic sampling period S, and the switching threshold parameter ε.
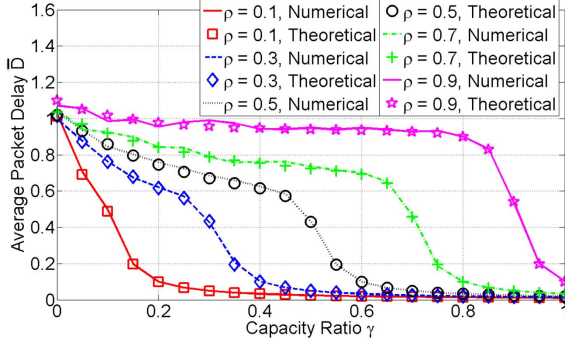
Fig. 2. Average packet delay $\overline{D}$ vs. capacity ratio γ, with $S = 1$ and $\varepsilon = 0$.
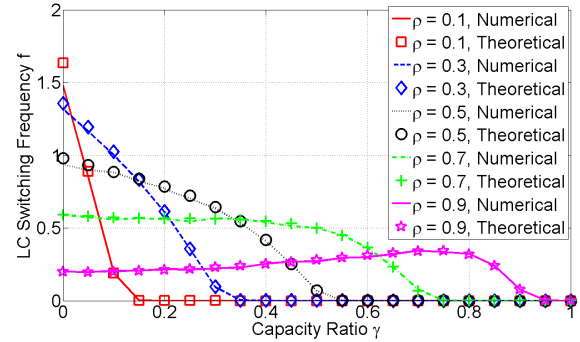

Fig. 3. LC switching frequency f vs. capacity ratio γ, with $S = 1$ and $\varepsilon = 0$.

A. Capacity Ratio between Master and Slave LCs

In this Subsection, we fix $S = 1$, $\varepsilon = 0$ to investigate the impacts of $\gamma = \mu_s/\mu_m$ on $\overline{D}$, f, and η, defined in Eqns. (9-11). Figs. 2-4 plot the results from both theoretical calculations and numerical simulations. It can be seen that the analytical results match well with the numerical ones. Fig. 2 shows the impact of γ on average packet delay $\overline{D}$. The results indicate that $\overline{D}$ has a sudden decrease when $\gamma \to \rho$. This is because that when $\gamma \to \rho$, the slave LC's capacity μ_s is catching up with the traffic load ρ. The impact of γ on LC switching frequency f shown in Fig. 3 indicates that f decreases with γ and becomes 0 when $\gamma > \rho$. Fig. 4 illustrates the results on energy efficiency improvement η. We observe that when $\gamma \to 1$, $\eta \to 0$. This can be explained as that when $\gamma = 1$, the master-slave configuration becomes a master-master configuration that is equivalent to the normal operation without any energy-saving. In the other extreme case when $\gamma = 0$, the system reduces to a single LC configuration with the sleeping-mode based energy-saving. Hence, when $\gamma \to 0$, η approaches to its maximum value $1 - \rho$. Notice that $\gamma \to 0$ also results in significant increases on both $\overline{D}$ and f as shown in Figs. 2-3. In between of these two extreme cases, η decreases slowly with γ until it joins the curve of $\eta = 1 - \gamma^{2/3}$ at $\gamma = \rho$.

Fig. 5 shows the energy-delay tradeoff with numerical simulation results. It can be seen that for different traffic loads, a reasonably good energy-delay tradeoff can be obtained at an optimal γ, as marked on the curves. Beyond this point, $\overline{D}$ increases rapidly for only a small amount of improvement on η.

B. Average Traffic Queue Sampling Period

We investigate the impacts of the average traffic queue sampling period, i.e., S, in this Subsection, with $\varepsilon = 0$ and ρ at 0.5 and 0.8. Fig. 6 illustrates the impact of S on the average packet delay $\overline{D}$. We observe that when $\gamma \to 0$, $\overline{D}$ almost equals to S. This is because that when $\gamma \to 0$, the capacity of the slave LC is negligible, and hence packets in the queue have to wait till the end of a sampling period to be transmitted on the master LC. As expected, when we fix γ and ρ, $\overline{D}$ increases with S. The impact of S on the LC
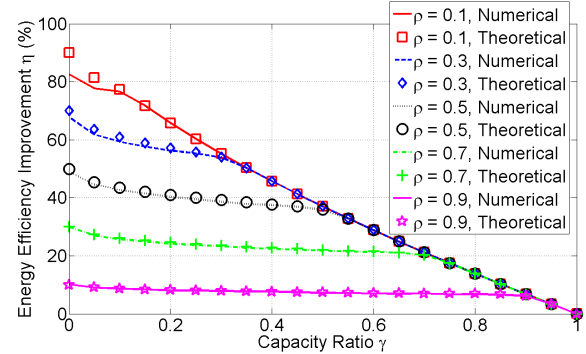

Fig. 4. Energy efficiency improvement η vs. capacity ratio γ, with $S = 1$ and $\varepsilon = 0$.

switching frequency f shows an opposite trend as in Fig. 7, and $f \to (1/S)$ when $\gamma \to 0$.

C. Switching Threshold Parameter

Switching a LC between working and sleeping modes too frequently can result in significant transition overheads [7]. We show in this Subsection that f can be reduced by adjusting the switching threshold parameter ε. With S fixed at 1, Figs. 8-9 illustrates the impact of ε on $\overline{D}$ and f, respectively. The curves suggest that f can be reduced by increasing ε, while
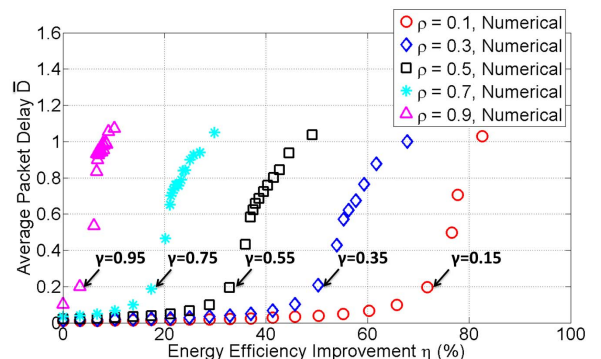

Fig. 5. Energy-delay tradeoff with $S = 1$ and $\varepsilon = 0$.
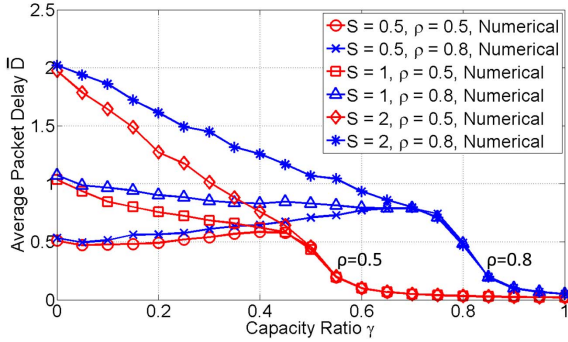
Fig. 6. Average packet delay $\overline{D}$ vs. capacity ratio γ, with various S and $\varepsilon = 0$.
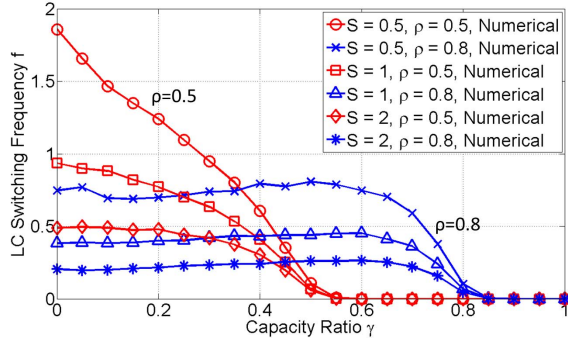
Fig. 7. LC switching frequency f vs. capacity ratio γ, with various S and $\varepsilon = 0$.

the average delay $\overline{D}$ would not be affected significantly.

V. CONCLUSION

We developed a traffic scheduling algorithm to explore the energy-saving capability of the master-slave LC configuration in a CMTS. In order to optimize the algorithm, the system was modeled using a two-dimensional Markov process to provide the analytical expressions of several performance metrics. Both theoretical and simulation results indicated that the
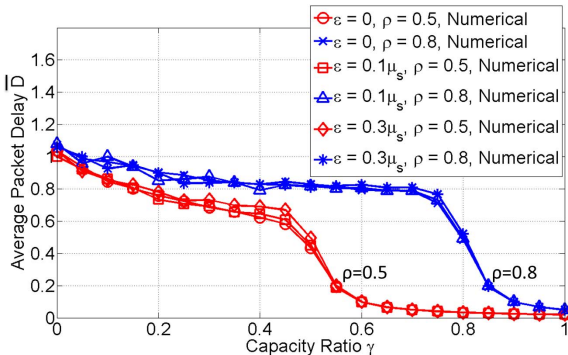
Fig. 8. Average packet delay $\overline{D}$ vs. capacity ratio γ, with $S = 1$ and various ε.
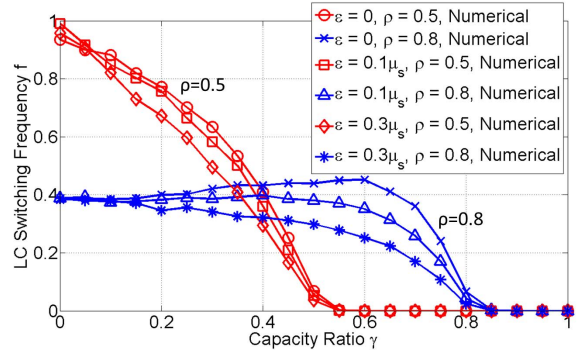
Fig. 9. LC switching frequency f vs. capacity ratio γ, with $S = 1$ and various ε.

proposed algorithm could achieve significant energy efficiency improvement, while keeping the average packet delay and LC switching frequency low.

REFERENCES

[1] J. Baliga, R. Ayre, K. Hinton, and R. Tucker, "Energy consumption in wired and wireless access networks," *IEEE Commun. Mag.*, vol. 49, no. 6, pp. 70–77, Jun. 2011.
[2] S. Videv and H. Haas, "Energy-efficient scheduling and bandwidth-energy efficiency trade-off with low load," in *Proc. of ICC 2011*, pp. 1–5, Jun. 2011.
[3] J. Zhang and N. Ansari, "Extending onu lifetime beyond 72 hours in EPON for emergency communications," in *Proc. of ICNC 2012*, pp. 287–291, Jan. 2012.
[4] P. Chowdhury, M. Tornatore, S. Sarkar, and B. Mukherjee, "Building a green wireless-optical broadband access network (WOBAN)," *J. Lightw. Technol.*, vol. 28, no. 16, pp. 2219–2229, Aug. 2010.
[5] I. Kamitsos, P. Tsiaflakis, H. Sangtae, and M. Chiang, "Stable sleeping in DSL broadband access: Feasibility and tradeoffs," in *Proc. of GLOBECOM 2011*, pp. 1–6, Dec. 2011.
[6] Z. Zhu, "Design energy-saving algorithms for hybrid fiber coaxial networks based on DOCSIS 3.0 standard," *J. Opt. Commun. Netw.*, vol. 4, no. 6, pp. 449–456, Jun. 2012.
[7] L. Ping *et al.*, "Energy-efficient scheduling and energy-delay tradeoff in green hybrid fiber-coaxial networks," in *Proc. of GLOBECOM 2012*, pp. 1–6, Dec. 2012.
[8] J. Cioffi, "Lighting up copper," *IEEE Commun. Mag.*, vol. 49, no. 5, pp. 30–43, May 2011.
[9] http://www.cablelabs.com/specifications/.
[10] http://www.cablelabs.com/cablemodem/specifications/specifications30.html.
[11] M. Parker and S. Walker, "Stochastic energy-efficiency optimization in photonic networking by use of master-slave equipment configurations," in *Proc. of ONDM 2012*, pp. 1–6, Apr. 2012.
[12] M. Garcia, D. Garcia, V. Garcia, and R. Bonis, "Analysis and modeling of traffic on a hybrid fiber-coax network," *J. Select. Areas Commun.*, vol. 22, no. 11, pp. 1718–1730, Nov. 2004.
[13] "High availability white paper," http://www.cisco.com/warp/public/cc/so/neso/ns269/hapwp_wp.pdf.
[14] R. Tucker, "Optical packet-switched WDM networks: a cost and energy perspective," in *Proc. of OFC 2008*, pp. 1–3, Mar. 2008.
[15] M. Neuts, *Matrix-Geometric solutions in stochastic models: an algorithmic approach*. Johns Hopkins University Press, 1981.